Inorg. Chem. **2008**, *47*, 3234−3242

Synthesis, Morphology, Structure, and Magnetic Characterization of Layered Cobalt Hydroxyisocyanates

Yi Du and Dermot O'Hare*

Chemistry Research Laboratory, Department of Chemistry, University of Oxford, Mansfield Road, Oxford, U.K. OX1 3TA

Received November 16, 2007

New layered pink cobalt hydroxyisocyanates have been prepared by controlled hydrolysis of aqueous solutions of $CoCl_2 \cdot 6H_2O$. $Co(OH)_{1.4}(NCO)_{0.6} \cdot 0.6H_2O$ (**1**) is formed when urea is used as the hydrolysis agent and mannitol as the stabilizer, while $Co(OH)_{1.25}(NCO)_{0.75} \cdot 0.2H_2O$ (**2**) is formed when the hydrolysis agent is changed to hexamethylenetetramine and NaOCN is added to the solution. IR spectroscopy of **1** and **2** indicates that the OCN^- is N-bonded to Co^{2+}. The X-ray powder data for **1** could be indexed using an intergrowth model consisting of both rhombohedral ($R\bar{3}m$ (166); $a = 3.2031(1)$ Å, $c = 23.6876(11)$ Å, hydrotalcite-like, $3R_1$) and hexagonal ($P\,63/mmc$ (194); $a = 3.2005(2)$ Å, $c = 15.8303(5)$ Å, Manasseite-like, $2H_1$) polytypes. Rietveld refinement of the X-ray powder data was performed using a two polytype model and 30% random substitution of the OH^- ions by OCN^-. Although it is less crystalline, the XRD data for **2** can be indexed using a rhombohedral-symmetry cell with unit cell parameters, $a = 3.158$ Å and $c = 21.57$ Å. Both **1** and **2** exhibit magnetically ordered ground states with a saturation magnetization of ca. 2.0 μ_B. The magnetization data is consistent with 3D ferromagnetic ordering of edge-share octahedral-Co^{2+} layers with effective spin $S' = {}^1/_2$.

Introduction

Cobalt (II) hydroxides are well-known to crystallize in two polymorphic forms, α and β. The β-form has a brucite-like structure consisting of a closed-packed array in which the divalent metal ion is located in an octahedral site generated by six hydroxyl oxygen atoms, while the α-cobalt hydroxides are reported to be isostructural with hydrotalcite-like compounds consisting of positively charged $Co(OH)_{2-x}$ layers and charge balancing anions (e.g., NO_3^-, CO_3^{2-}, Cl^-, etc.) in the interlayer gallery.[1] It is of major interest to both chemists and physicists due primarily to the rigidity of the metal–oxygen network brought about by the μ_3-OH and the edge sharing octahedral.[2] The chemical interest mainly stems from the intercalation chemistry[3,4] and the potential applications of these materials as heterogeneous catalysts;[4,5] however, significant interest from materials chemists and physicists has been prompted by the observation of long-range interlayer magnetic interactions in a range of organically pillared cobalt hydroxides and hydroxysulfates.[2,6–12]

To date, the synthesis of crystalline single-phase samples of α-cobalt hydroxides has proven to be difficult because the α-phase is metastable and typically transforms rapidly to the β-phase during synthesis or upon storage in strong alkaline media.[13–15] Many attempts have been made to prepare the α-cobalt hydroxide by electrochemical and

* E-mail: dermot.ohare@chem.ox.ac.uk. Fax: +44 1865 272690. Tel: +44 1865 285130.

(1) Kamath, P. V.; Annal Therese, G. H.; Gopalakrishnan, J. *J. Solid State Chem.* **1997**, *128*, 38.
(2) Mohsen, B. S.; Vilminot, S.; Richard-Plouet, M.; Andre, G.; Mhiri, T.; Kurmoo, M. *Chem. Comm.(Cambridge, United Kingdom)* **2004**, 2548.
(3) Yamanaka, S.; Kawaji, H.; Hotehama, K.; Ohashi, M. *Adv. Mater.* **1996**, *8*, 771.
(4) Cavani, F.; Trifiro, F.; Vaccari, A. *Catal. Today* **1991**, *11*, 173.
(5) Didier, T.; Bernard, C. *CATTECH* **2003**, *7*, 206.
(6) Ben Salah, M.; Vilminot, S.; Andre, G.; Bouree-Vigneron, F.; Richard-Plouet, M.; Mhiri, T.; Kurmoo, M. *Chem. Mater.* **2005**, *17*, 2612.
(7) Forster, P. M.; Tafoya, M. M.; Cheetham, A. K. *J. Phys. Chem. Solids* **2004**, *65*, 11.
(8) Rabu, P.; S., A.; Legoll, P.; Belaiche, M.; Drillon, M. *Inorg. Chem.* **1993**, *32*, 2463.
(9) Demessence, A.; Rogez, G.; Rabu, P. *Chem. Mater.* **2006**, *18*, 3005.
(10) Takada, T.; Bando, Y.; Kiyama, M.; Miyamoto, H.; Sato, T. *J. Phys. Soc. Jpn.* **1966**, *21*, 2726.
(11) Drillon, M.; Panissod, P.; Rabu, P.; Souletie, J.; Ksenofontov, V.; Gulich, P. *Phys. Rev. B* **2002**, *65*, 104404.
(12) Rujiwatra, A.; Kepert, C. J.; Claridge, J. B.; Rosseinsky, M. J.; Kumagai, H.; Kurmoo, M. *J. Am. Chem. Soc.* **2001**, *123*, 10584.
(13) Liu, Z.; Ma, R.; Osada, M.; Takada, K.; Sasaki, T. *J. Am. Chem. Soc.* **2005**, *127*, 13869.
(14) Gaunand, A.; Lim, W. L. *Powder Technol.* **2002**, *128*, 332.

10.1021/ic702260s CCC: $40.75 © 2008 American Chemical Society
Published on Web 03/13/2008

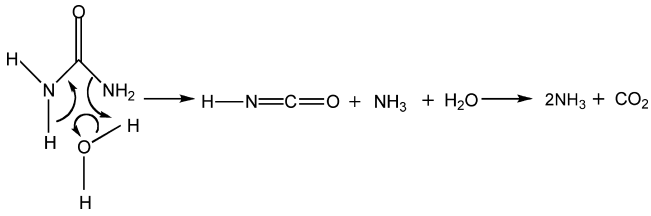

Figure 1. Reaction scheme for the hydrolysis of urea and the production of HNCO.

chemical synthesis including urea and ammonia precipitation as well as sonication-assisted methods.[2,15–18] Unfortunately, most of the α-cobalt hydroxides synthesized are either poorly crystalline and/or adopt a turbostratically disordered structure,[15–18] in which the layers are randomly oriented about the *c*-axis. In addition, the crystallites rarely adopt a uniform or well defined morphology but typically occur as aggregates.[13] There is one structural report of green-colored single-crystal α-cobalt hydroxides which was prepared using hexamethylenetetramine (HMT) as the hydrolysis agent.[13] Rietveld refinement of the powder XRD suggests a structural model involving tetrahedral cobalt coordination.[19] Although a pink-colored form of an α-cobalt hydroxide phase has been reported[17] no structural data on this material has been published. Therefore, it is of interest to search for novel routes for the preparation of crystalline materials with well-defined, uniform particle size and morphology. In this paper, we have studied the use of both urea/mannitol and hexamethylenetetramine/NaOCN mixtures to prepare layered cobalt hydroxyisocyanates. In these reactions, the slow hydrolysis of urea or hexamethylenetetramine controls the pH, while mannitol acts as a stabilizer to prevent transformation to a *β*-type cobalt hydroxide.

Experimental Section

Synthesis of $Co(OH)_{1.4}(NCO)_{0.6}\cdot 0.6H_2O$ (1). Pink color $Co(OH)_{1.4}(NCO)_{0.6}\cdot 0.6H_2O$ (**1**) was prepared using a homogeneous precipitation method. $CoCl_2\cdot 6H_2O$ (0.47 g), mannitol (0.03 g), and urea (6 g) were dissolved in 200 cm^3 of a 9:1 mixture of deionized water and ethanol to give the final concentrations of 10, 1, and 500 mM, respectively. The deionized water was purged with N_2 overnight and the addition was carried out with stirring under an ambient pressure N_2 atmosphere. The reaction solution was then heated to 90 °C in the absence of magnetic stirring. After 4 h at 90 °C, a suspension containing bright pink microcrystals formed. The precipitate was filtered and washed thoroughly with deionized water, anhydrous ethanol, and acetone several times and, finally, air-dried at room temperature to give an isolated yield of 60%. The material has uniform hexagonal platelet-like crystal morphology.

Synthesis of $Co(OH)_{1.25}(NCO)_{0.75}\cdot 0.2H_2O$ (2). $Co(OH)_{1.25}(NCO)_{0.75}\cdot 0.2H_2O$ (**2**) was prepared using a similar homogeneous precipitation method as outlined for (**1**). $CoCl_2\cdot 6H_2O$ (0.47 g), NaOCN (0.78 g) and hexamethylenetetramine, HMT (2 g) were dissolved in 200 cm^3 of a 9:1 mixture of N_2 saturated deionized water and ethanol to give the final concentrations of 10, 60 and 60 mM, respectively. The reaction solution was then heated to 90 °C in the absence of magnetic stirring under a N_2 atmosphere. After 2 h at 90 °C, a suspension containing bright pink crystals formed. The precipitate was filtered and washed thoroughly with deionized water, anhydrous ethanol, and acetone several times and, finally, air-dried at room temperature to give an isolated yield of 70%. The resulting crystals were pale pink in color with a uniform flower-like crystal morphology.

Material Characterization. IR spectra of the samples as KBr discs were recorded over the range of 600−4000 cm^{-1} on a Mattson Galaxy Series 6020 FT-IR spectrometer. Sixteen scans were recorded with a scan resolution of 8 cm^{-1}. Elemental analysis (EA) was performed by the analytical services department of the Inorganic Chemistry Laboratory, Oxford University. C, H, and N contents were calculated by quantitatively digesting the sample through oxidative combustion. Other elements were analyzed using inductively coupled plasma (ICP) atomic emission spectroscopy. Thermogravimetric analysis (TGA) were carried out on a Rheometric STA-1500H machine. The sample (ca. 10 mg) was mounted in a corundum crucible and heated at a rate of 1 °C min^{-1} between 30 and 700 °C under a flow of argon. Powder X-ray diffraction (XRD) patterns were recorded on a PANalytical X'Pert Pro instrument in reflection mode with Cu Kα radiation ($\lambda = 1.54178$ Å). The accelerating voltage was set at 40 kV with 40 mA current. The diffractometer was equipped with X'Celerator detector. Scan rates were typically 0.002° s^{-1} (continuous scan, step size 0.008°, time per step 500s). Scanning electron microscopy was performed on a JSM 840F at 5 kV, samples coated with Pt before analysis. High-resolution transmission electron microscopy (HRTEM) and selected area electron diffraction (SAED) were performed on a JEOL 4000EX at 400 kV. A JEOL 2000FX instrument operating at 200 kV was used for energy dispersive X-ray (EDX) analysis. Samples were dispersed in ethanol and loaded onto copper grids supporting Formvar film. Magnetic measurements were made using a Quantum Design MPMS-5 SQUID magnetometer. The susceptibility was determined in an applied field of 1 kG/5G after cooling of the sample in both zero applied field (ZFC) and the measuring field (FC). The saturated moment and hysteresis loop was measured at 2 K for ZFC in fields up to 50 kG.

Results

Synthesis. The homogeneous precipitation method has been used previously to prepare crystalline layered cobalt hydroxides.[13] In this paper, we have exploited the slow hydrolysis reaction of urea in basic solution (Figure 1) as a method to enable us to control the nucleation and growth of highly ordered, phase-pure cobalt hydroxyisocyanates. Addition of a mixture of $CoCl_2\cdot 6H_2O$, mannitol, and urea to a nonstirred, deionized water/ethanol mixture at 90 °C results in the phase pure synthesis of pink, highly crystalline, hexagonal platelets of cobalt hydroxyisocyanate in 60% yield. Our detailed characterization including elemental analysis (Table 1), IR, thermogravimetric analysis (TGA), EDX (Supporting Information Figure S1), X-ray diffraction, and TEM are all consistent with a formulation of $Co(OH)_{1.4}(NCO)_{0.6}\cdot 0.6H_2O$ (**1**). We postulate that isocyanic acid (OCNH) formed as a result of the hydrolysis of urea (Figure 1) reacts to displace some of the OH^- ions from the coordination sphere of the Co^{2+} ions forming cobalt isocyanate (Co−NCO) bonds. At present it is unknown whether

(15) Xu, Z.; Zeng, H. *Chem. Mater.* **1999**, *11*, 67.
(16) Xu, R.; Zeng, H. *Chem. Mater.* **2003**, *15*, 2040.
(17) Rajamathi, M.; Kamath, P. V. *Int. J. Inorg. Mater.* **2001**, *3*, 901.
(18) Rajamathi, M.; Kamath, P. V.; Seshadri, R. *Mater. Res. Bull.* **2000**, *35*, 271.
(19) Ma, R.; Liu, Z.; Takada, K.; Fukuda, K.; Ebina, Y.; Bando, Y.; Sasaki, T. *Inorg. Chem.* **2006**, *45*, 3964.

Table 1. Summary of Elemental Microanalysis Data

compound	morphology	elemental composition obs (calc) % N	C	H	Co	formula
1	hexagonal platelets	6.56(7.06)	5.75(6.06)	2.22(2.21)	49.9(49.6)	$Co(OH)_{1.4}(NCO)_{0.6}\cdot 0.6H_2O$
2	flower	8.78(9.10)	7.99(7.80)	1.55(1.45)	50.2(51.0)	$Co(OH)_{1.25}(NCO)_{0.75}\cdot 0.2H_2O$

NCO for OH substitution happens in solution before condensation of the $Co(OH)_2$ layers or as a result of NCO^- intercalation in solid $Co(OH)_2$. Nevertheless, the color of the material and the XPS data (Supporting Information Figure S2) strongly suggests that the sample contains exclusively octrahedrally coordinated Co^{2+} ions.

Surprisingly, if the controlled precipitation reaction is performed in the absence of urea and mannitol but instead we use hexamethylenetetramine (HMT) as the hydrolysis agent in the presence of sodium cyanate (NaOCN), then the flower-like morphology crystals of a different layered cobalt hydroxide phase are isolated in 70% yield. On the basis of analytical and spectroscopic data, this material may be formulated as $Co(OH)_{1.25}(NCO)_{0.75}\cdot 0.2H_2O$ (**2**).

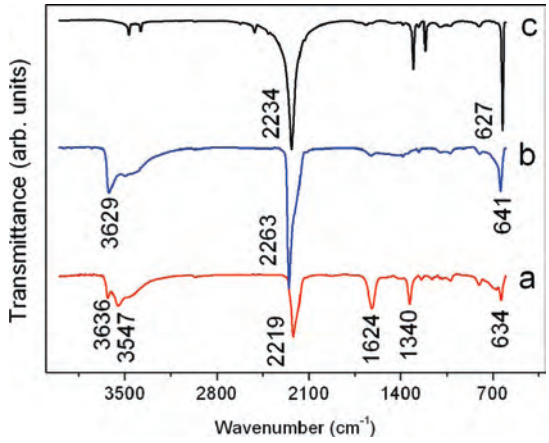

Figure 2. FT-IR spectra of (a) **1**, (b) **2**, and (c) NaNCO. .

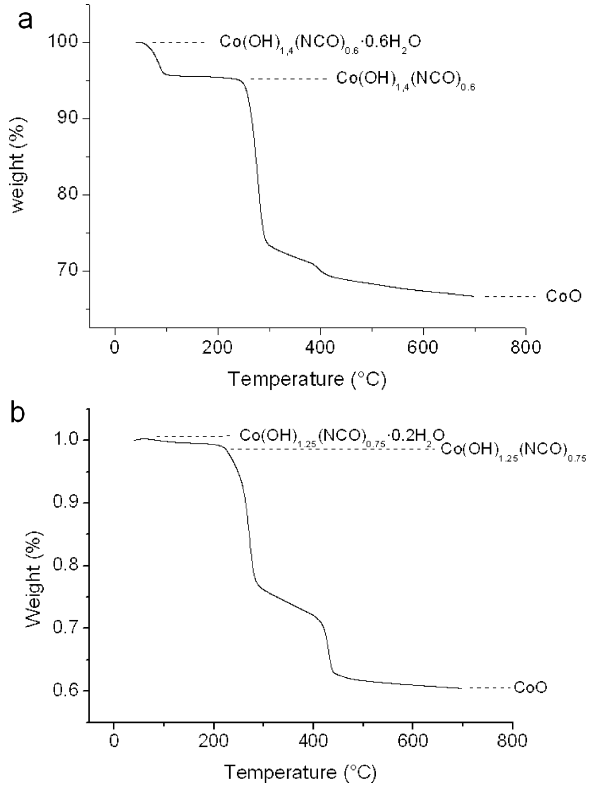

Figure 3. TGA traces for (a) **1** and (b) **2**.

IR Spectroscopy. Vibrational spectroscopy has proved to be the principal method for studying the existence and bonding mode of the OCN anion in metal complexes. Three normal IR active vibrational modes for the free OCN ion are the antisymmetric stretching (υ_{CN}), the pseudosymmetric stretching (υ_{CO}) and the bending (δ_{NCO}). They occur at 2160(s), (1296 and 1204)(m), and (635 and 628)(m) cm^{-1}, respectively.[20–22] The positions of these bands are shifted upon coordination to metal centers. The FT-IR of **1** and **2** are shown in Figure 2 together with the IR of sodium cyanate (NaOCN) for reference. The presence of the OCN^- ion in both **1** and **2** is clearly shown by the absorptions at ca. 2219, 634 and 2263, 641 cm^{-1} for **1** and **2**, respectively, which may be assigned to (υ_{CN}).[20–26] However, the OCN^- anion, is potentially ambidentate and one may distinguish if this anion is nitrogen bonded (i.e., isocyanate: −NCO) or oxygen bonded (i.e., cyanate: −OCN) to a metal center by reference to the frequency of the remaining weaker pseudosymmetric stretching υ_{CO} mode.[27,28] The published literature indicates for metal isocyanate complexes (N-bonded) only a single band assigned to υ_{CO} is observed with a positive shift compared to free OCN to ca. 1350–1300 cm^{-1}.[22,25,29,30] For metal cyanates (O-bonded) a negative shift in frequency is predicted for the υ_{CO}. For **1**, we clearly resolve a band at 1340 cm^{-1} which we assign to υ_{CO} of a Co−NCO moiety. Unfortunately, we do not observe a similar absorbance in the IR spectrum in **2**; however, this mode is commonly reported to be a weak feature. On balance, we favor a similar Co−NCO coordination for **2**. This is supported by a review of the literature on OCN^- containing metal complexes which indicates that almost all first row transition metals contain

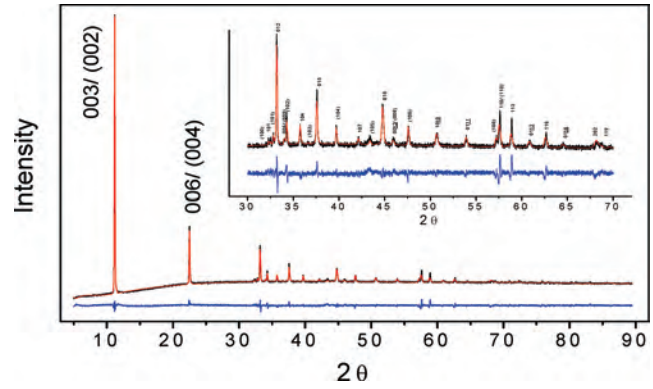

Figure 4. Results of Rietveld refinement for **1**: experimental (black), calculated (red), and the difference spectrum (blue) XRD data. The inset shows a magnification of the high 2θ region. Miller indices for relatively strong Bragg reflections are indicated for rhombohedral and hexagonal (in bracket) polytypes, respectively.

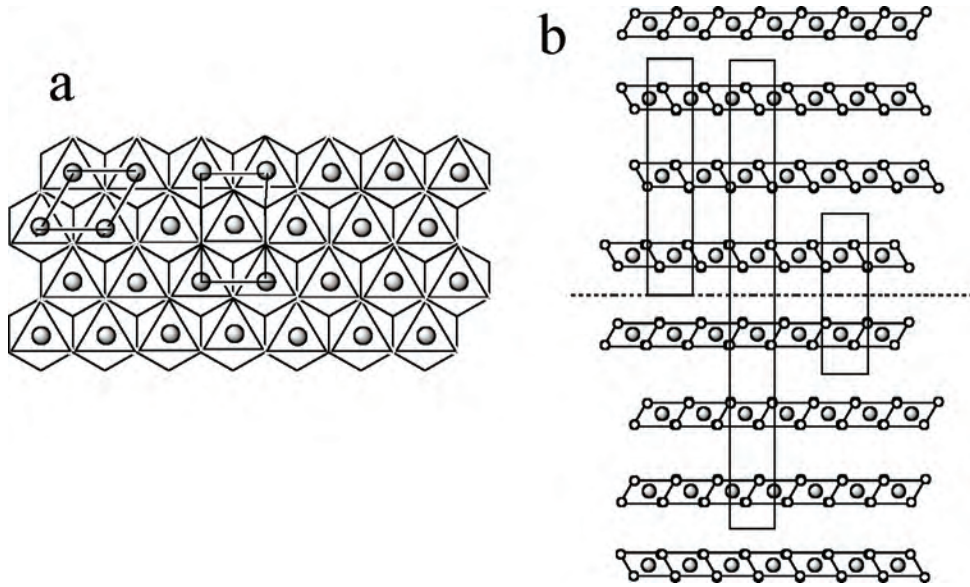

Figure 5. Various possible unit cell choices for **1**. (a) Intralayer ($a \approx a_0$, $c \approx 2a_0 \sin 60°$). (b) Interlayer ($b \approx 6c_0$) related to the rhombohedral/ hexagonal model (a, b, and c are cell parameters from the $Pmm2$ space group, a_0 and c_0 are cell parameters from the $R\bar{3}m$ space group).

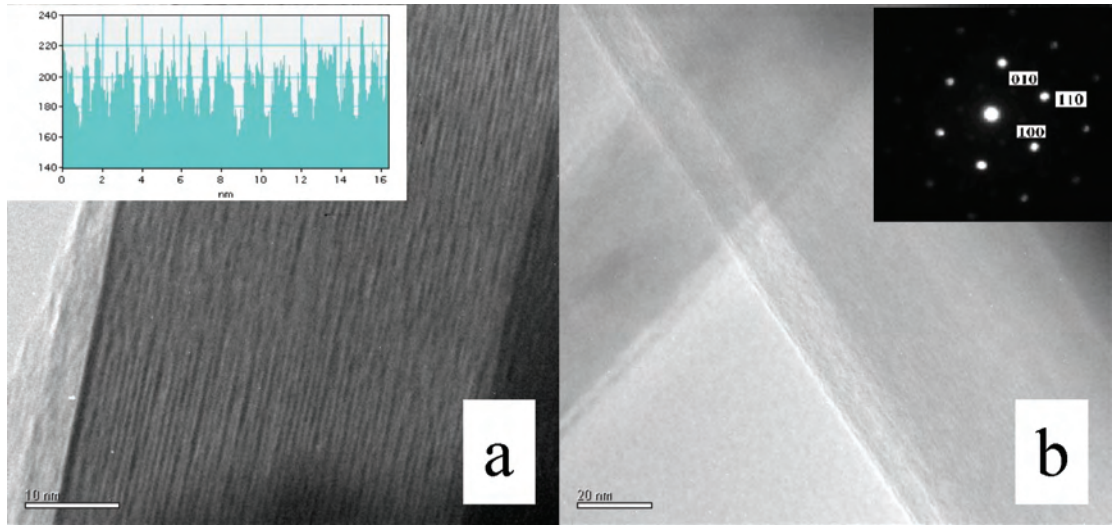

Figure 6. TEM images of **1**: (a) perpendicular to c-axis, (b) parallel to c-axis.

Table 2. Summary of the Crystallographic Data for **1** Based on a Mixed Phase Refinement[a]

	rhombohedral model	hexagonal model
space group	$R\bar{3}m$ (166)	$P63/mmc$ (194)
a (Å)	3.2031(1)	3.2005(2)
c (Å)	23.6876(11)	15.8303(5)
V (Å^3)	210.47(1)	140.43(1)
Z	3	2
calc. formula sum.	$Co(OH)_{1.4}(NCO)_{0.6}\cdot 0.6H_2O$	$Co(OH)_{1.4}(NCO)_{0.6}\cdot 0.6H_2O$
phase fractions	73.3(10)%	26.7(10)%

[a] Fitted $R_{wp} = 1.10\%$, $R_p = 0.76\%$, $-BnkR_{wp} = 2.11\%$, $R_p = 1.60\%$, and $\chi^2 = 3.29$.

N-bonded OCN ligands.[22,31] In 2006, Faus and co-workers reported they were the first to structurally characterize a

Table 3. Atomic Positions and Thermal Parameters for **1** Based on an Intergrowth of Two Polytypes of Rhombohedral and Hexagonal Symmetry

Rhombohedral Model						
atom	site	x	y	z	SOF	U [Å^2]
Co1	3a	0	0	0	1	0.0195(11)
O1/N1	6c	0	0	0.62337(13)	0.7/ 0.3[a]	0.023(2)[b]
C1	6c	0	0	0.5722(5)	0.3[a]	0.023(2)[b]
O2	6c	0	0	0.5214(5)	0.3[a]	0.023(2)[b]
O3	6c	0	0	0.5013(6)	0.3[a]	0.089(6)
Hexagonal model						
atom	site	x	y	z	SOF	U [Å^2]
Co1	2a	0	0	0	1	0.0195(11)
O1/N1	4f	1/3	2/3	0.06509(17)	0.7/0.3[a]	0.021(2)[b]
C1	4f	1/3	2/3	0.1420(7)	0.3[a]	0.021(2)[b]
O2	4f	1/3	2/3	0.2186(8)	0.3[a]	0.021(2)[b]
O3	4f	1/3	2/3	0.2510(8)	0.3	0.074(6)

[a] Statistically disordered with 70% OH^- and 30% OCN^-, $SOF(O_3) = SOF(H_2O) = 0.3$. [b] Thermal parameters constrained to be equal.

(20) Mavis, B.; Akinc, M. *Chem. Mater.* **2006**, *18*, 5317.
(21) Talismanova, M. O.; Sidorov, A. A.; Novotortsev, V. M.; Aleksandrov, G. G.; Nefedov, S. E.; Eremenko, I. L.; and Moiseev, I. I. *Russian Chem. Bull., Int. Ed.* **2001**, *50*, 2251.
(22) Martinez-Lillo, J.; Armentano, D.; De Munno, G.; Lloret, F.; Julve, M.; Faus, J. *Inorg. Chim. Acta* **2006**, *359*, 4343.

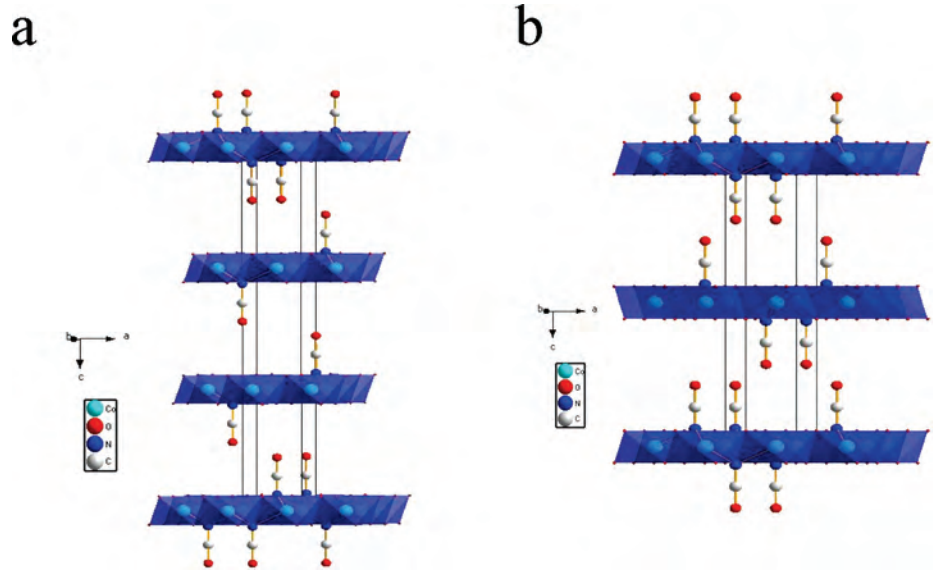

Figure 7. Structural model of **1** generated from Rietveld refinement based on an intergrowth model of two polytypes of rhombohedral (a) and hexagonal symmetry (b). Co, O, N, and C are presented by light blue, red, dark blue, and white spheres, respectively. The average occupancy for the hydroxyl and NCO groups is 70% and 30%, respectively.

Table 4. Selected Bond Lengths and Angles for **1** Based on an Intergrowth of Two Polytypes of Rhombohedral and Hexagonal Symmetry

rhombohedral model		hexagonal model	
Co1−O1/N1	2.11463(3)	Co1−O1/N1	2.11574(7)
N1−C1	1.21136(2)	N1−C1	1.21768(2)
C1−O2	1.2045(13)	C1−O2	1.21225(2)
Co1−N1−C1	119.010(1)	Co1−N1−C1	119.143(1)

M−OCN complex.[22] The bending vibration of interlayer water molecules gives rise to absorptions at 1650 cm^{-1} in layered double hydroxide (LDH) spectra.[32] Therefore, we assign the 1624 cm^{-1} absorbance for **1** to intercalated water which is in agreement with the XRD, elemental analysis, and TGA data. Both the TGA and elemental analysis data for **2** suggests that **2** contains almost no water and this supported the absence of an equivalent band in the IR spectrum. Finally, the absence of any absorptions ca. 1500 cm^{-1} in the IR data of in either **1** or **2** suggest that no CO_3^{2-} ions are present either as impurity phases or by cointercalation.

Thermogravimetric Analysis. TGA was performed on **1** and **2** in order to investigate the number of water molecules cointercalated and to gain insight into the decomposition processes that occur. TGA traces for both samples are given in Figure 3. Both TGA traces share a similar shape. Mass loss occurs in two/three stages. The initial mass loss of ca. 1–5% begins at temperatures below 100 °C, which corresponds to the loss of interlayer water, to give the dehydrated materials $Co(OH)_{1-x}(NCO)_x$ ($x = 0.6$ and 0.75). Further decomposition events we ascribe to the dehydration of the layers and decomposition of the OCN^- ligands, to finally give a calcined product which has a powder XRD pattern corresponding to CoO. We observe a slight inconsistency between the percentage water in these materials as measured by elemental analysis and TGA which we think this is due to a small variation from sample to sample in the amount of absorbed water or cointercalated water. The figures given in Table 1 are the best fit to the elemental analysis data.

Structural Characterization. The X-ray powder diffraction pattern of **1** is shown in Figure 4. At first inspection, the pattern has the features expected for a rhombohedral symmetry α-type cobalt hydroxide similar to that reported in the literature.[13,19] For example, two prominent low-angle reflections at $d = 7.83$ and 3.92 Å could be assigned to 003 and 006 Bragg reflections of the hydrotalcite-like phase with

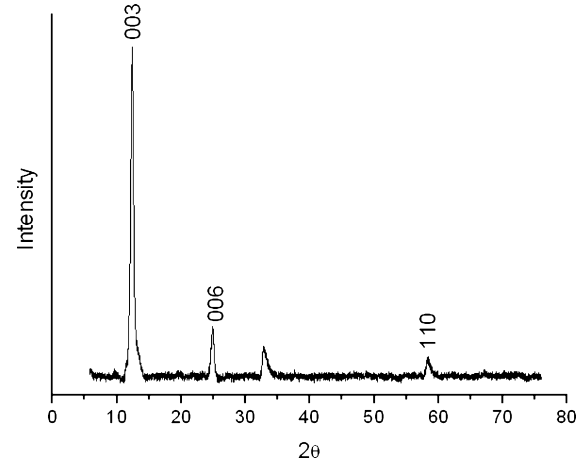

Figure 8. XRD pattern for **2**.

(23) Sato, K.; Yoshinari, T.; Kintaichi, Y.; Haneda, M.; Hamada, H. *Appl. Catal. B: Environ.* **2003**, *44*, 67.
(24) Nelson, J. N. *J. Chem. Soc. A* **1969**, 1597. a. S. M.
(25) Sabatini, A.; Bertini, I. *Inorg. Chem.* **1965**, *4*, 959.
(26) Maki, A.; Decius, J. C. *J. Chem. Phys.* **1958**, *28*, 1003.
(27) Mavis, B.; Akinc, M. *J. Am. Ceram. Soc.* **2006**, *89*, 471.
(28) Carbacho, H.; Ungerer, B.; Contreras, G. *J. Inorg. Nuc. Chem.* **1970**, *32*, 579.
(29) Anderson, S. J.; Brown, D. S.; Finney, K. J. *J. Chem. Soc., Dalton Trans.* **1979**, 152.
(30) Fawcett, J.; Peacock, R. D.; Russell, D. R. *J. Chem. Soc., Dalton Trans.* **1987**, 567.
(31) D'Agnano, A.; Gargano, M.; Malitesta, C.; Ravasio, N.; Sabbatini, L. *J. Electron Spectrosc. Relat. Phenom.* **1991**, *53*, 213.
(32) Williams, G. R.; O'Hare, D. *Solid State Sci.* **2006**, *8*, 971.

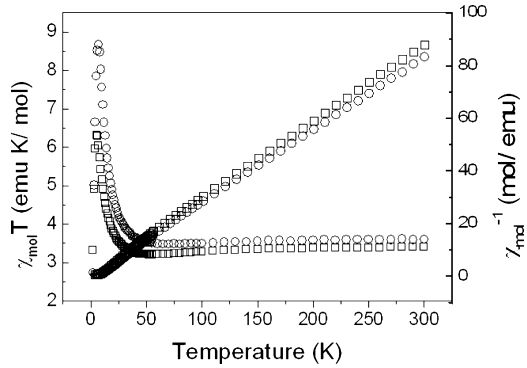

Figure 9. Plots of $\chi_{mol}T$ vs T and χ_{mol}^{-1} vs T following zero-field cooling between 2 and 300 K for (**1** □), (**2** ○).

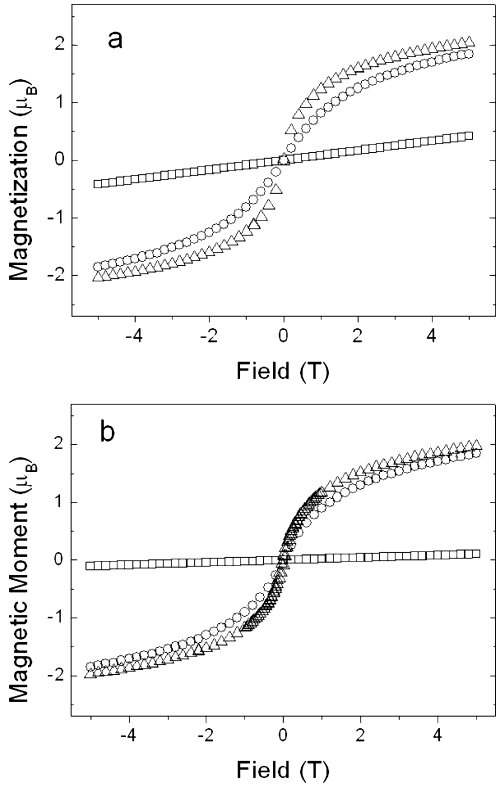

Figure 10. (a) Plot of molar magnetization (M) vs field (T) for **1** at 70 (□), 10 (○), and 2 K (Δ). (b) Plot of molar magnetization (M) vs field (T) for **2** 70 (□), 10 (○), and 2 K (Δ).

unit cell parameter, $c = 23.52$ Å (hydrotalcite-like, $3R_1$).[33] The Bragg reflection at $d = 1.60$ Å could be indexed as 110 which allows us to determine the unit cell parameter $a = 3.20$ Å. However, on closer inspection, we find that not all the observed Bragg reflections could be indexed on this unit cell. For example, two prominent low-angle reflections at $d = 2.60$, 2.25, 1.90 Å could only be indexed to the 102, 104, and 106 Bragg reflections of a hexagonal symmetry cell with $c = 15.68$ Å (manasseite-like, $2H_2$),[33] the 110 Bragg reflection at $d = 1.60$ Å allows us to deduce hexagonal unit cell parameter $a = 3.20$ Å (see bracketed reflections inset in Figure 4). Using these two unit cells, it is possible to index the entire X-ray powder diffraction pattern. However, the X-ray powder diffraction (XRD) data may also be fully indexed using an orthorhombic unit cell (*Pmm*2 (25)) with lattice constants $a = 3.1823(5)$, $b = 47.130(8)$, and $c = 5.5125(10)$ Å, This orthorhombic cell is related to the rhombohedral cell ($a \approx a_0$, $c \approx 2a_0 \sin 60°$, $b \approx 6c_0$, where a_0 and c_0 are the approximate lattice parameters of the rhombohedral/ hexagonal unit cell) as shown in Figure 5. We have carefully considered the validity of both models and have performed a parallel refinement using the orthorhombic cell model. Since the orthorhombic cell does not index any additional observed reflections and the final agreement factors for the refinement using the orthorhombic cell model are no better even though we have greater number of least-squares variables and the electron microscopy (see below), we have chosen to report the results obtained using the intergrowth model below.

Furthermore compound **1** was also been studied by high-resolution transmission electron microscopy (HRTEM) and selected area electron diffraction (SAED) with a view to probing the symmetry of the crystalline domains. Figure 6a and b shows TEM images of **1**. The corresponding selected area electron diffraction (SAED) pattern (inset in Figure 6b) shows a diffraction pattern which can be indexed as a two-dimensional in-plane hexagonal lattice. This implies that the platelets are lying on their {001} zone axis direction. The HREM image (Figure 6a) shows lattice fringes separated by 0.76 nm. On the basis of all our microscopy data, we believe it is best to consider the structure of **1** as an intergrowth of rhombohedral and hexagonal symmetry polymorphs.

In order to build trial models for structural refinement, we then considered the nature of individual cobalt hydroxide layers and the isocyanate location. It is possible that the structure may be analogous to hydrotalcite-like layered double hydroxides,[15] in which the positive charge originates from partial substitution of divalent metal cations by trivalent cations in a brucite-like octahedral layer. However, this is not the case here because of the lack of Co^{3+} in the α-form. From the X-ray photoemission spectroscopy (XPS) spectrum, we observe no photoemission from a Co^{3+} ion (see Supporting Information Figure S2). Furthermore, the existence of Co^{3+} would result in a gray/black colored sample rather than the pure pink color of our product.

Another possibility is the existence of additional Co^{2+} cations at interstitial (tetrahedral) sites. Recently, the Sasaki group[19] have reported the results of a Rietveld refinement on a green color Cl^- ion intercalated α-cobalt hydroxide. Their model was based on a rhombohedral symmetry phase with the Co^{2+} cations in both octahedral and tetrahedral coordination sites. The refinement clearly demonstrated that one-fifth to one-sixth of the Co^{2+} in octahedral sites were replaced by pairs of tetrahedrally coordinated Co^{2+} on either side of the hydroxide plane; the material can be represented by a structure formula $[Co^{octa}_{0.828}Co^{tetra}_{0.348}(OH)_2]^{0.348+}$-$Cl_{0.348}\cdot 0.45H_2O$. In their example, the material has a characteristic green color. Cobalt complexes typically fall into two general groups; pink−red octahedral complexes and intensely blue tetrahedral complexes. Green can be identified as a mixture of tetrahedral and octahedral complexes.

(33) Ramesh, T. N.; Rajamathi, M.; Kamath, P. V. *J. Solid State Chem.* **2006**, *179*, 2386.

Table 5. Summary of the Magnetic Data for **1** and **2**

samples	μ_{eff} (μ_B)	C (emu K mol^{-1})	θ (K)	M_{SAT} (μ_B)	coercive field (Oe)	remanent magnetization (μ_B)
$Co(OH)_{1.4}(NCO)_{0.6}\cdot 0.6H_2O$ (**1**)	5.26	3.46	−5.11	∼2.00	80	0.02
$Co(OH)_{1.25}(NCO)_{0.75}\cdot 0.2H_2O$ (**2**)	5.38	3.62	−2.72	∼2.00	270	0.09

Therefore, we believe that our pink cobalt hydroxyisocyanates materials are entirely composed of octahedral cobalt centers.

Finally, a third model involving hydroxyl ion substitution was considered.[1] In this model, the isocyanate anions are incorporated into the octahedral layers by replacing some of the OH^- ions and directly coordinated to the Co^{2+} cations. In this model, the cobalt centers all remain as octahedrally coordinated 2+ cations. The longer rod-like OCN^- would expand the interlayer distance to ∼8 Å. Thus, a novel structure model based on 30% hydroxyl substitution by OCN^- is proposed. A Rietveld refinement was performed on a rigid body fragment model with soft constraints on the bond lengths.

The summary of the refinement parameters is given in Table 2, final atomic positions and thermal parameters are presented in Table 3, and the experimental, calculated, and the difference XRD patterns for **1** are shown in Figure 4. The structural model generated from the results of the Rietveld refinement for **1** are shown in Figure 7. The structure consists of sheets of cobalt octahedra and these layers are stacked along the *c*-direction. We see no evidence on any OCN^- ordering in either the electron diffraction or X-ray diffraction data. The OCN^- ions are arranged perpendicular to the layer planes. Each cobalt octahedra is linked through either edge-sharing hydroxyl or isocyanate ions. A μ_3-NCO ligand has been observed previously for Co^{2+} ions[21] and other metal compounds.[22,33,34] In the refinement, a rigid body model was first employed and a composite O/N atom was used corresponding to the chemical composition with a fixed Co^{oct}−O/N = 2.11 Å. The N═C and C═O bond lengths in the NCO^- ligand were also fixed at 1.20 Å, which are close to the values found of 1.179(5) and 1.190(5) Å for a μ^2-NCO ligand bridging two Co^{2+} centers.[19,21] Moreover, an oxygen atom was introduced in each phase model at (0, 0, 0.498) and (1/3, 2/3, 0.251), respectively, with a fractional occupancy set to model the amount of cointercalated water.

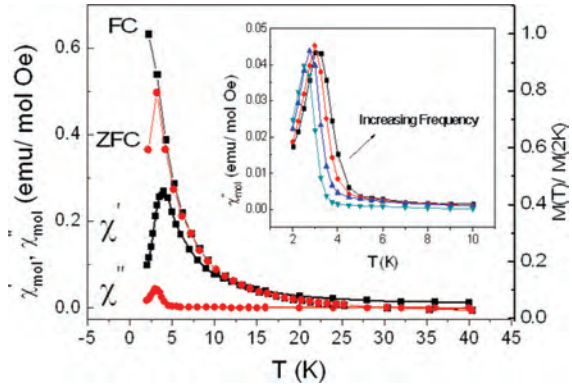

Figure 11. Tempereature dependence of the dc magnetization in ∼5 Oe and the in- an out-of-phase ac magnetization for **1** between 2 and 40 K under an oscillating magnetic field of 3.5 Oe. (inset) Frequency dependence of ac susceptibility (χ'') for **1** between 2 and 10 K under an oscillating magnetic field of 3.5 Oe.

The phase fractions of the rhombohedral and hexagonal symmetry polymorphs were also allowed to refine, and this resulted in a composition of ca. 70% rhombohedral and 30% hexagonal forms. We managed to refine the atomic position with separate successive cycles. Selected bond lengths and angles for **1** are given in Table 4. The agreement indices and the Estimated Standard Deviations (esds) on the refined parameters reflect that this refinement is less than ideal. Even after all our efforts, we still observe some poor agreements between the observed and calculated data between 50 and 60° in 2θ. However, we would like to highlight that this does represent a rare example of a quantitative refinement of the X-ray powder diffraction data from a hydrotalcite-like phase prepared at low temperature.

The XRD data for **2** (Figure 8) indicates that this phase is less crystalline than **1**. Nevertheless, the XRD data may be indexed using a single rhombohedral hydrotalcite-like cell with unit cell parameters, a = 3.158 and c = 21.57 Å. The full-width at half-maximum (fwhm) of the 003 Bragg reflection for **2** is 0.267° which is significantly larger than 0.094° found for the equivalent 003 reflection in the rhombohedral phase in **1**. These data are clearly not of sufficient quality or angular range to enable us to perform a structural refinement.

Direct Current Magnetic Measurements. The molar magnetic susceptibility of **1** and **2** was studied as a function of temperature (2−300 K) and applied magnetic field (0–5 T). A plot of the temperature dependence of $\chi_{mol}T$ for both **1** and **2** after cooling in zero field is shown in Figure 9. Both **1** and **2** behave as paramagnets above 50 K. Above 50 K, the magnetic susceptibilities can be fitted to the Curie–Weiss law (Figure 9) with effective molar magnetic moments μ_{eff} = 5.26 and 5.38 μ_B and negative Weiss constants of −5.1 and −3.6 K for **1** and **2**, respectively. The observed effective magnetic moments are higher than the spin-only value predicted for an $S = {}^3/_2$ ion (μ_{SO} = 3.87 μ_B), but they do fall within the experimental range (4.7–5.4 μ_B) found for octahedral Co^{2+}which would be expected to adopt a $^4T_{1g}$ ground state.[9,36,37]

On cooling below 50 K, $\chi_{mol}T$ for both **1** and **2** exhibit a shallow minimum before rapidly increasing at low temperature. This slight decrease in $\chi_{mol}T$ has been observed by Rabu and Drillon et al., for β-$Co(OH)_2$ and $Co_2(NO_3)(OH)_3$, and was ascribed to spin–orbit coupling effects for Co^{2+} ion stabilizing a Kramers doublet ground-state and/or competing

(34) Nicola, C. D.; Effendy; Fazaroh, F.; Pettinari, C.; Skelton, B. W.; Somers, N.; White, A. H. *Inorg. Chim. Acta* **2005**, *358*, 720.
(35) Luo, J.; Zhou, X. G.; Weng, L. H.; Hou, X. F. *Acta Crystallogr. Sect. C* **2003**, *59*, 519.
(36) Kurmoo, M.; Kumagai, H.; Hughes, S. M.; Kepert, C. J. *Inorg. Chem.* **2003**, *42*, 6709–6722.
(37) Drillon, M.; Panissod, P. *J. Magn. Magn. Mater.* **1998**, *188*, 93.

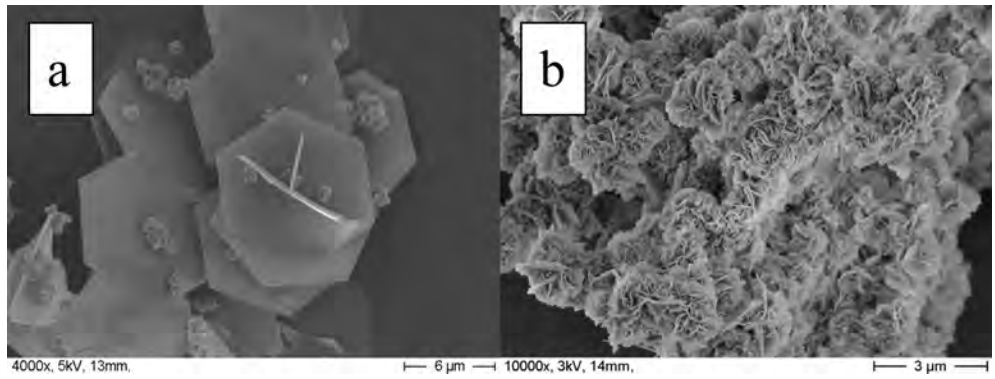

Figure 12. (a) SEM image of **1**. (b) SEM image of **2**. A trace amount (<1%) of cobalt impurity phase was observed in **1**.

in-plane magnetic interactions between Co^{2+} moments.[8] The large increase in $\chi_{mol}T$ at low temperature suggests the onset of a 3D ordered state.[11,38,39]

The field dependence of the molar magnetization, $M(H)$, for **1** at three different temperatures is shown in Figure 10a. At 70 K, the plot of M vs H is linear as expected for a paramagnet. Least squares fitting of $M(H)$ at 70 K for an $S = {}^3/_2$ ion allows us to determine an average isotropic g-value for the Co^{2+} ions of 2.64. Below 10 K, the M vs H data deviate from the behavior predicted by the Brillouin function. At 2 K, the $M(H)$ curve rises rapidly with increasing field and tends toward a saturation magnetization (M_{SAT}) of approx 2.0 μ_B. At 2 K, **1** exhibits a narrow hysteresis loop with a coercive field of 80 Oe. Similar $M(H)$ curves can be observed for **2** as shown in Figure 10b. For **2**, an isotropic $<g>$ value of 2.72 may be deduced from the least-squares fitting of $M(H)$ at 300 K. At 2 K, the $M(H)$ curve tends toward a similar saturation magnetization of ~2.00 μ_B. The summary of dc magnetic data for both **1** and **2** are in Table 5. The saturation magnetization (M_{SAT}) is predicted to be $gS\,\mu_B$ for an ensemble of ferromagnetically aligned spins (S). Thus for **1** and **2**, we would expect M_{SAT} of 3.96 and 4.08 μ_B, respectively, if the Co^{2+} ions adopt a well defined $S = {}^3/_2$ ground-state at low temperature. However, lower than expected saturation magnetization values has been observed previously for several magnetically ordered layered Co^{2+} hydroxides. This has been ascribed to 3D ferromagnetic ordering of the Co^{2+} sites in which the octahedral Co^{2+} ions adopt a ground-state Kramers doublet giving an effective $S' = {}^1/_2$.[35,39]

Layers of cobalt hydroxides such as β-$Co(OH)_2$ and $Co_2(NO_3)(OH)_3$ exhibit ferromagnetic inplane interactions. At low temperature in the ordered state, these compounds exhibit metamagnetic behavior.[8] The magnetic properties of several organic intercalated layered cobalt hydroxides with large interlayer separations have been studied in detail by Kurmoo, Drillon, Kepert, and Rosseinsky.[11,35–38] These materials show ferromagnetic coupling between these widely spaced layers, and this has been ascribed to long-range dipolar interactions.[9,11,36,40] For **1** or **2**, we see no evidence of any metamagnetism which would be indicated by a sudden change the in the gradient of the $M(H)$ curves; the data is consistent with both ferromagnetic inplane and interplane interactions.

Alternating Current Magnetic Measurements. The temperature dependence of ac magnetic susceptibility for **1** was measured in the temperature range 2–40 K under an oscillating magnetic field of 3.5 Oe (under a near-zero dc field of 5 Oe) (Figure 11). Spontaneous magnetic ordering for 3D magnets is characterized by a discontinuous jump in dc magnetization which coincides with the peak in the in-phase ac magnetization and to the nonzero out of phase ac magnetization. The sharp peaks in both real (in phase) and imaginary (out of phase) components of the ac susceptibilities are taken to be indicative of a ferromagnetic 3D ordering transition. The Curie temperature, T_C, of the sample, was determined to be 4 and 3 K for **1** and **2** (ac susceptibility measurement for **2** is not shown) by inspection of the real and imaginary components of the ac susceptibilities (Figure 11).

The frequency dependence of imaginary (χ'') components of the magnetic susceptibility for **1** between 2 and 10 K is shown inset in Figure 11. The maximum in χ'' occur ca. 3 K but becomes smaller and shifts to higher temperatures with increasing frequency. The real component, χ' varies with temperature in the same way as χ'' but with much larger susceptibility. Below 5 K, χ'' rises from zero to a maximum at 3 K. The observed nonzero χ'' below 4 K confirms the transition to a magnetically ordered ground-state with a net spontaneous magnetization. The spontaneous magnetization could be further proved by a sharp increase of dc magnetization and by a peak in both the in- and out-of-phase components of the ac magnetization as shown in Figure 10.[35,39]

Crystal Morphology. Figure 12a shows the SEM images of **1** following crystallization at 90 °C. The sample is composed of uniform hexagonal crystalline platelets with widths in the range 6–7 μm and thickness ca. 20 nm. The SEM image of **1** shows the presence of a small amount of an cobalt impurity phase. In contrast, the SEM image of **2** (Figure 12b) which also forms at 90 °C in the presence of NaNCO yields flower-like morphology crystallites with a radius around 0.4−1 μm. The difference in morphology may be ascribed to the fact that a larger number of smaller nuclei

(38) Williams, D. L.; Smith, D. W.; Stoufer, R. C. *Inorg. Chem.* **1967**, *6*, 590.
(39) Figgis, B. N.; Nyholm, R. S. *J. Chem. Soc.* **1954**, 12.
(40) Kurmoo, M. *Chem. Mater.* **1999**, *11*, 3370.

nucleate during the condensation of **2**, and these aggregate to form spherical structures.

Conclusions

A series of pink layered cobalt hydroxyisocyanates (hexagonal sheet platelets/flower-like structures) have been synthesized and characterized. IR spectroscopy shows that **1** and **2** both contain the N-bonded Co−NCO ligands, A Rietveld refinement has been performed for **1**. The structure is composed of layers of divalent cobalt(II) ions in octahedral coordination with 30% of hydroxyl replaced by OCN^- anions. The extended structure is best considered as an intergrowth of containing both approximately 70% rhombohedral and 30% hexagonal polytypes. Both **1** and **2** have 3D ferromagnetically ordered ground states with a net saturation magnetization corresponding to ordered Co^{2+} ions with an effective $S' = {}^1/_2$.

Acknowledgment. The authors thank Clarendon Scholarship Fund for financial support to Y.D. We thank Dr. H. Wang for XPS measurements.

Supporting Information Available: EDX for **1**; XPS spectrum of **1**. This material is available free of charge via the Internet at http://pubs.acs.org.

IC702260S